Composites Science and Technology 87 (2013) 103–110

Contents lists available at ScienceDirect

Composites Science and Technology

journal homepage: www.elsevier.com/locate/compscitech

Tough nanopaper structures based on cellulose nanofibers and carbon nanotubes

Michaela Salajkova [a,b], Luca Valentini [c], Qi Zhou [a,b,d], Lars A Berglund [a,b,*]

[a] Department of Fibre and Polymer Technology, Royal Institute of Technology, SE-100 44 Stockholm, Sweden
[b] Wallenberg Wood Science Center, Royal Institute of Technology, SE-100 44 Stockholm, Sweden
[c] Civil and Environmental Engineering Department, University of Perugia, 051 00 Terni, Italy
[d] School of Biotechnology, Royal Institute of Technology, AlbaNova University Centre, SE-106 91 Stockholm, Sweden

ARTICLE INFO

Article history:
Received 8 April 2013
Received in revised form 7 June 2013
Accepted 15 June 2013
Available online 2 July 2013

Keywords:
A. Nanocomposite
A. Functional composite
B. Mechanical properties
D. Atomic force microscopy
D. Scanning electron microscopy

ABSTRACT

Carbon nanotube (CNT) nanocomposites based on CNT in a polymer matrix typically have low strain to failure in tensile loading. Furthermore, mixing of more than a few percent of CNT with either molten thermoplastics or monomers in bulk often results in agglomeration of CNT. Here, multiwalled CNT (MWCNT) are mixed with nanofibrillated cellulose (NFC) in aqueous suspension and filtered into tough nanopaper structures with up to 17 wt% of MWCNT commingled with NFC nanofibrils. Carbon nanotubes were surface treated with a surfactant, and homogenous suspensions of carbon nanotubes in water miscible with the NFC suspension was obtained. NFC/CNT nanopaper structures were characterized for porosity using mercury displacement, and studied by FE-SEM and AFM. Mechanical properties were tested in uniaxial tension and electrical conductivity was measured. The processing route is environmentally friendly and leads to well-mixed structures. Thin coatings as well as thicker films can be prepared, which show a combination of high electrical conductivity, flexibility in bending and high tensile strength.

1. Introduction

Nanostructured multiphase materials are interesting since they have potential for dramatically improved materials performance, and can also provide multifunctional characteristics. In order to successfully introduce such materials in large-scale industrial applications, several challenges need to be addressed. Perhaps the most important one is to disperse nanoparticles homogeneously on small scale. Another challenge is that many nanoparticles are quite expensive. Recently, nanofibrillated cellulose (NFC), in the form of cellulose nanofibers disintegrated from wood pulp, has been widely studied [1–3]. NFC may successfully address both challenges; good nanoparticle dispersion and low cost. Another advantage is that NFC forms nanofiber networks of high mechanical performance [1].

NFC can be homogeneously dispersed in water, as facilitated by charged groups on the surface of NFC, such as anionic NFC prepared by carboxymethylation [4] or by TEMPO-mediated oxidation (TEMPO stands for 2,2,6,6-tetramethyl-1-piperidinyloxyl, free radical that catalyzes the oxidation of primary alcohol groups of cellulose in aqueous media) [5–7] or cationic NFC prepared by disintegration of wood pulp that was cationized by glycidyltrimethylammonium chloride [8]. Another dispersion approach is to adsorb a hydrophilic polymer to the individual nanofibers [9]. Each nanofiber is coated and becomes separated from its nanofiber neighbors. This can result in a favorable combination of modulus, strength and toughness in the resulting nanocomposites [10]. The favorable price of wood-based NFC is due to the cost advantage of chemical wood pulp but also due to the recent development of pretreatment methods, which reduce energy requirements for the mechanical disintegration of the NFC from the wood pulp fibers. Pretreatment with enzymes [11,12] or by above mentioned chemical methods [4–8] are good examples. NFC can bond wood fibers and is used as a strength enhancement additive in paper and board materials [13]. Addition of NFC can also allow a larger amount of low-cost inorganic fillers in paper and board structures. The reason is that NFC forms strong and tough networks. Strengthening mechanisms are discussed in studies of clay nanopaper materials of very high inorganic content [14–16].

Apart from inorganic fillers, functional carbon-based nanoparticles are of interest. Graphene nanosheets particles can be processed as aqueous dispersions, and this development represents major progress [17]. For carbon nanotubes (CNT), the advantage of papermaking approaches has been demonstrated [18]. Challenges to address with CNT nanocomposites include CNT

* Corresponding author. Address: Wallenberg Wood Science Center, Teknikringen 56, SE-100 44 Stockholm, Sweden. Tel.: +46 8 790 81 18; fax: +46 8 790 61 66.
E-mail address: blund@kth.se (L.A Berglund).

0266-3538
http://dx.doi.org/10.1016/j.compscitech.2013.06.014

agglomeration and low CNT content limited by the preparation procedure. In the present study we prepare mixed aqueous suspensions of NFC and CNT and proceed to nanopaper preparation by filtration.

In previous work, large and smooth sheets of NFC-montmorrilonite (MTM) clay nanopaper were prepared by a paper-making approach [14]. The content of clay could be as high as 90% by weight. The material demonstrated high modulus, tensile strength and strain to failure despite the high inorganic content [15]. The reason is that NFC forms a continuous matrix phase in the form of a strong and tough nanofibrous network. If chitosan is added so that a two-phase matrix is obtained, the processing time is shortened since dewatering is faster. Also, some improvements in mechanical properties are observed through chitosan-NFC synergies [16]. A similar processing route based on filtering and drying of aqueous suspensions will be investigated in the present study.

The development of smart paper technology is of great interest as an application area for NFC. The goal is improved properties and the addition of new functionalities to mechanically functional paper structures of low cost. Electrically conductive paper is of particular interest in electromagnetic interference shielding, electronic circuits, as strain gauges [19], active matrix displays, high strength cables and substrates [20] and loudspeaker membranes [21].

There are previous attempts to mix CNT with cellulose. Anderson et al. [20] prepared composite paper based on micro-scale wood pulp and single-walled carbon nanotubes at a content of up to 35% by weight. Prior to that, Fugetsu et al. [22] considered electrical conductivity and reported a percolation concentration of 8.32% by weight multiwall CNT (MWCNT) for MWCNT/wood pulp. Oya and Ogino [23] combined traditional Japanese papermaking process with CNT and prepared electrically conductive paper. The resulting paper structures showed signs of heterogeneity, as is expected when the cellulose fiber phase is tens of microns in diameter and several mm in length.

Bacterial cellulose (BC) combined with CNT has been prepared either by adsorption of the CNT on bacterial cellulose in hydrogel form [19,24–26] or by synthesis of BC in a CNT dispersion [27,28]. NFC from wood pulp offers the advantage of much lower cost than BC and the potential for large scale applications. Composite materials based on regenerated cellulose and CNT have also been prepared [29,30]. This requires the use of solvents, which are not needed in the present papermaking route.

The objective of the present study is to develop a water based processing route for preparation of commingled NFC/CNT nanopaper structures. A commingled structure means that the NFC and CNT nanofibers are intimately mixed. This requires surface modification of the CNT in order to disperse the CNT in water. The goal is to form a stable NFC/CNT dispersion. Furthermore, the nanostructure of the dried, commingled nanopaper network will be characterized. Mechanical and electrical properties will be studied as a function of composition. The present study is a developed version of a chapter in a licentiate thesis [31]. Recently, Koga et al. [32] published a study on blends between TEMPO-NFC and single wall carbon nanotubes. The present study is more focused on deformation behaviour of this class of materials, in particular the ductility of the porous nanopaper structure.

2. Experimental section

2.1. Materials

A commercial softwood pulp was used as native cellulose fibers. Never-dried sulphite pulp was provided by Nordic Paper. The cellulose content was 86% and the rest was mostly hemicelluloses. The degree of polymerization of cellulose was 1200. TEMPO (2,2,6,6-tetramethyl-1-piperidinyloxyl, free radical, 98%, Aldrich), sodium bromide (99%, Alfa Aesar), sodium hypochlorite (14%, GPR Rectapur, VWR) and sodium hydroxide (98%, Reagent, Sigma–Aldrich) were used without further purification. Multi-walled carbon nanotubes (Elicarb®, purity 70–90%) were provided by Thomas Swan and were purified with nitric acid (65%, Scharlau) and hydrochloric acid (37%, ACS, Merck) prior use. Nonylphenol POE-10 phosphate ester (STEPFAC 8170) was provided by Stepfan Company, Northfield, IL, USA.

2.2. Preparation of cellulose nanofibrils (NFC)

Cellulose nanofibrils were prepared by TEMPO-mediated oxidation of wood pulp according to method described by Saito et al. [5]. Briefly, the cellulose fibers were suspended in water containing TEMPO and sodium bromide. The TEMPO-mediated oxidation was started by adding the desired amount of the sodium hypochlorite solution and was continued at room temperature while stirring. The pH was kept at 10 by adding sodium hydroxide until no further sodium hydroxide consumption was observed. The TEMPO-oxidized cellulose was thoroughly washed with water by filtration. After the treatment, approximately 1% TEMPO-oxidized fiber suspension was disintegrated by a homogenization process with a Microfluidizer M-110EH (Microfluidics Ind., USA). Resulting suspension of microfibrillated cellulose (NFC) was stored at 4 °C before use.

2.3. Purification of multi-walled carbon nanotubes

Multi-walled carbon nanotubes were purified prior to use. It is well known that 3 M nitric acid is very effective at dissolving metal particles. On the other hand 5 M hydrochloric acid is suitable to dissolve metal oxide [33]. Therefore, the crude material was stirred in 3 M nitric acid and refluxed for 12 h at 60 °C. After that, MWCNT were suspended and refluxed in 5 M hydrochloric acid solution for 6 h at 120 °C [24].

2.4. Preparation of multi-walled carbon nanotubes suspension

Purified MWCNT were dispersed in water using acid phosphate ester of ethoxilated nonylphenol. Typically, 2% solution of surfactant (20 mg/mL) was used and the concentration of MWCNT was 5 mg/mL. After sonication with Ultrasonic processor (Sonisc Vibracell, VCX 750, Sonic&Materials, USA) equipped with 13 mm tip at 30% of the maximum power, stable suspension without any agglomerates was obtained.

2.5. Nanopaper preparation

Suspension of NFC was diluted to approximately 0.1 wt% and dispersed using shear forces (Ultra Turrax T18 basic, IKA Werke GmbH & Co. KG, Germany) for 5 min at 13,500 rpm. MWCNT suspension was added drop wise until desired MWCNT content (0.5–16.7 wt%) was obtained. Suspension was sonicated and stirred with magnetic stirrer overnight in order to obtain homogenous distribution of MWCNT in the cellulose nanofibrils network. After that, water was removed by filtration on a glass filter funnel (7.2 cm in diameter) using filter membrane (0.22 μm GV, Milipore, USA). Obtained wet cake was dried at 93 °C and vacuum for 10–20 min in sheet former (Rapid Kothen, RK3A-KWT PTI, Germany). Control samples containing only NFC (0% control) and NFC/4.8 wt% surfactant (4.8% control) were prepared using the same procedure. Resulting nanopaper sheets had 7 cm diameter and thickness 25 and 50 μm.

2.6. Characterization

Morphology of the nanopaper was observed using field emission scanning electron microscopy (FE-SEM). The specimen were fixed on a metal stub using colloidal graphite and coated with thin layer of gold–palladium coating using Cressington 208HR sputter coater. Hitachi S-4800 scanning electron microscopy operated at low acceleration voltage (1–1.5 kV) and short working distance was used to capture secondary electron images of the surface of the specimen.

Atomic force microscopy (AFM) was used to study detailed nanostructure of the material. The surfaces of the specimens were imaged with tapping-mode AFM (Multimode IIIa, Veeco Instruments, Santa Barbara, CA). Topographic (height) and phase images were recorded under controlled air conditions (23 °C and 50% relative humidity). RTESP silica cantilevers (Veeco, tip radius 8 nm and typical spring constant 40 N/m – values provided by manufacturer) were oscillated close to resonance frequency. The scan size was 1 μm^2. No further image processing except flattening was made.

Mechanical properties of the nanopaper were investigated using tensile test. Specimens of 40 mm length, 25 μm thickness and 5 mm width were tested using Universal Material Testing Machine Instron 5566 equipped with 100 N load cell. A cross-head speed of 4 mm/min which corresponds to an initial strain rate of 10%/min was used and the stress–strain curves were recorded. The experiment was performed under controlled air conditions of 23 °C and 50% relative humidity. Specimens were equilibrated under the same conditions for 2 days. The results are based on data collected from 7 specimens and the standard deviations were calculated.

Density of the nanopapers was determined using mercury displacement method [34]. The samples were weighed both in the air ($m_{Sample(air)}$) and when submerged in mercury ($m_{Sample(Hg)}$). The density of the samples (ρ_{Sample}) was calculated from (1) and the porosity (P) was calculated using Eq. (2), assuming the density of cellulose to be 1500 kg/m^3 and density of carbon nanotubes to be 2100 kg/m^3 [35]. Weight fractions of cellulose and MWCNT are represented by w_{cell} and w_{MWCNT}.

$$\rho_{Sample} = \rho_{Hg} \cdot m_{Sample(air)} / (m_{Sample(air)} - m_{Sample(Hg)}) \quad (1)$$

$$\text{Porosity } (\%) = [1 - \rho_{Sample} / (w_{cell} \cdot \rho_{cell} + w_{MWCNT} \cdot \rho_{Sample})] \cdot 100 \quad (2)$$

Electrical conductivity of the nanopaper was measured using a Keithley 6517B Electrometer/High Resistivity Meter together with a Keithley 8089 Resistivity Test Fixture. Using this test fixture, surface resistivity in the range of 10^3–10^{17} Ω can be measured.

3. Results and discussion

3.1. Structural characterization

In order to prepare commingled NFC/CNT nanopaper structures from aqueous solution, it is critical to have CNT stably dispersed in the NFC water suspension. A surfactant, nonylphenol polyoxyethylene (10) phosphate ester (abbreviated as NPPE), was used to modify the hydrophobic CNTs. Previous work by Heux and colleagues has shown that this surfactant can be used to coat the surface of cellulose whiskers and effectively aid their dispersion in organic solvents and poly(propylene) [36–38]. This surfactant can also improve the dispersion of cellulose whiskers in polylactic acid (PLA) [39]. As shown in Fig. 1a, unmodified MWCNT agglomerated and precipitated immediately after dispersion in water. In contrast, Fig. 1b demonstrates a homogenous and stable suspension of MWCNT (5 mg/mL) in water. It was obtained simply by addition of MWCNT into 20 mg/mL NPPE water solution followed by sonication for 10 min. NFC was prepared with a carboxylate content of 1.5 mmol/g. The carboxylate functionality contributes to NFC dispersion and suspension stability. However, without addition of NPPE, MWCNT precipitated out of the NFC water suspension (Fig. 1c). In contrast, a stable dispersion of MWCNT in NFC water suspension (Fig. 1d) was achieved by using MWCNT modified with NPPE. The reason is the strong repulsive dispersion force between the carboxylic group on the surface of NFC and the phosphate group on NPPE modified MWCNT. The NFC/MWCNT suspension was stable and formed no visible agglomerates during storage at room temperature for more than 6 months.

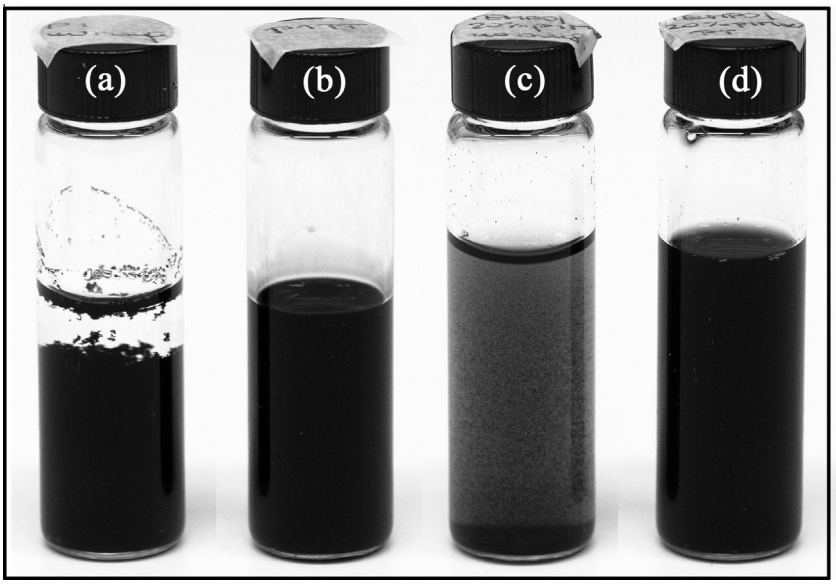

Fig. 1. Photography of: MWCNT suspension (5 mg/mL) in water without (a) and with 20 mg/mL NPPE surfactant (b) MWCNT suspension mixed with NFC suspension in water without (c) and with (d) NPPE surfactant (concentration is 0.1 mg/mL for NFC and 0.01 mg/ml for MWCNT; this corresponds to a nanocomposite composition of 9.1% MWCNT and 90.9% NFC (by weight).

NFC/CNT nanopaper structures with MWCNT content in the range of 0.5–16.7 wt% were prepared from the aqueous suspension mixtures of NPPE modified MWCNT and NFC [14]. Such technique enables thorough mixing of the suspension prior filtration. This is a considerable advantage compared to previous studies of CNTs mixed with bacterial cellulose pellicles [19,24], where the structure cannot be well controlled. FE-SEM micrographs and AFM phase images of nanopaper structures are presented in

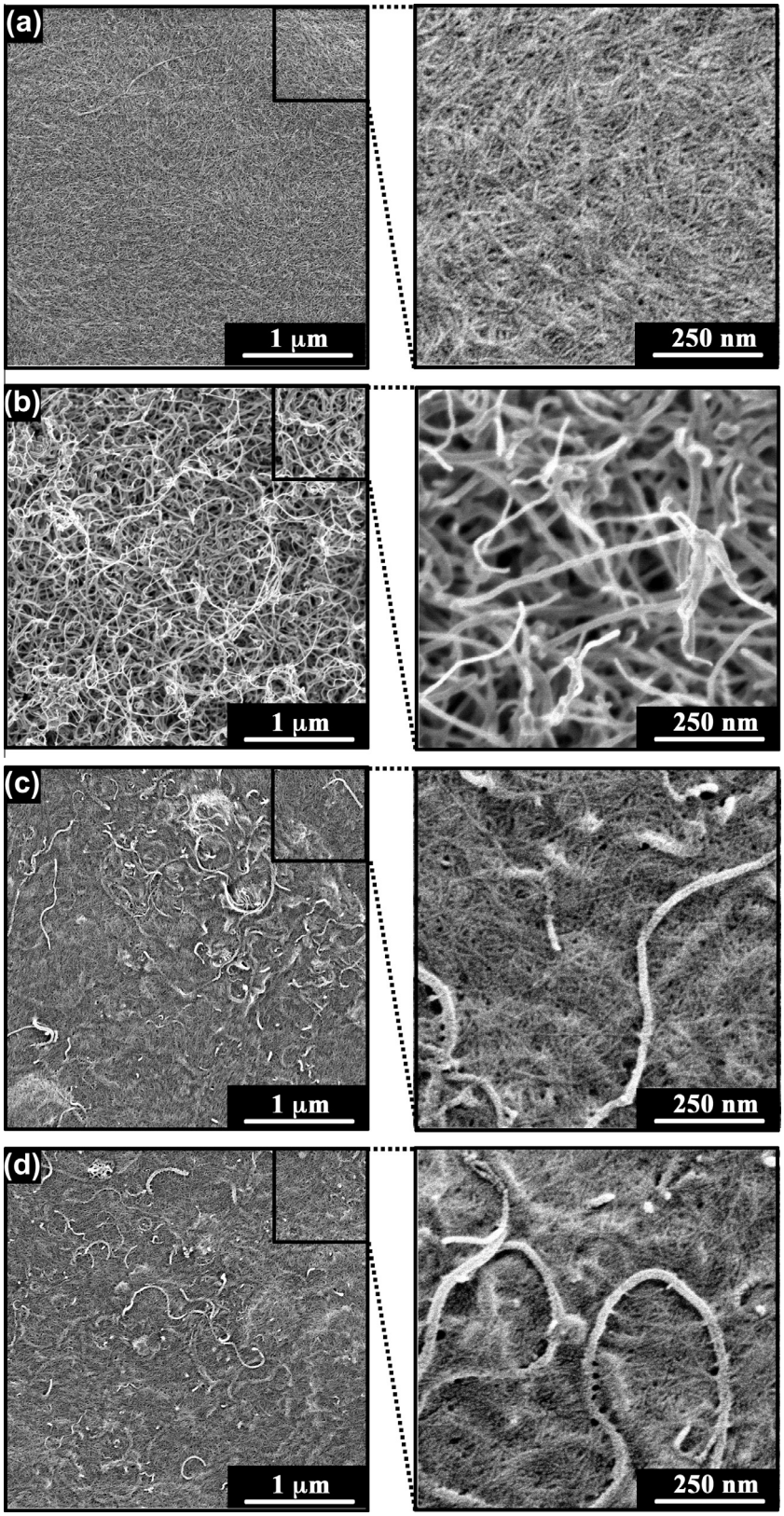

Fig. 2. FE-SEM micrographs of (a) NFC nanopaper, (b) NPPE modified MWCNT, (c) top surface and (d) bottom surface of NFC/CNT nanopaper containing 9.1 wt% MWCNT.

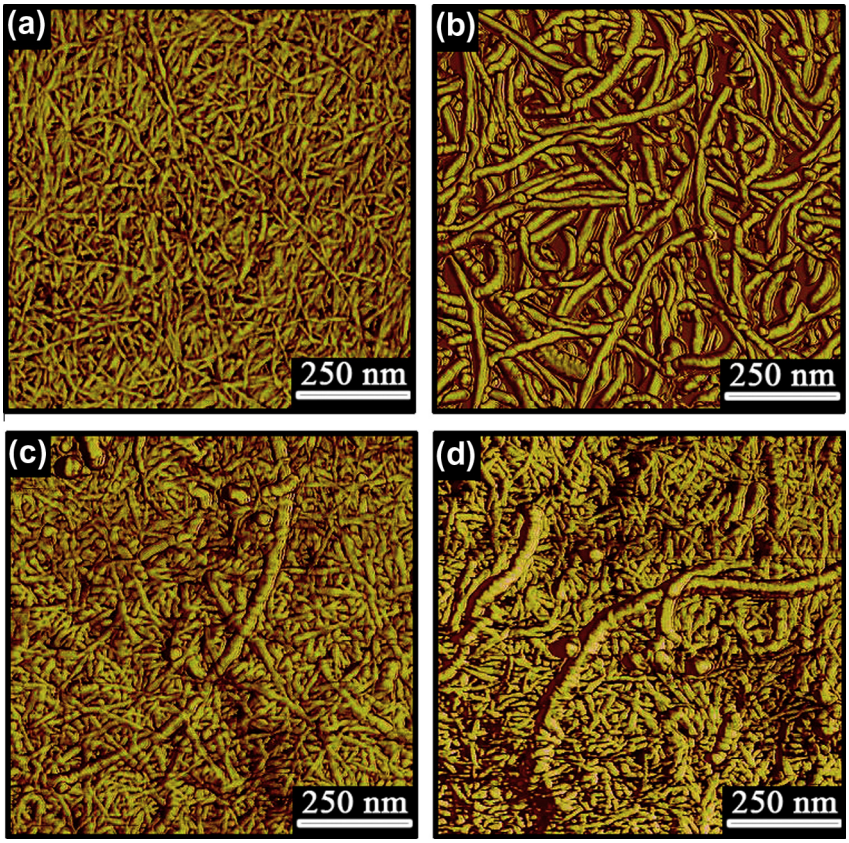

Fig. 3. AFM phase images of (a) control sample of NFC nanopapers, (b) control sample of MWCNT, (c) top surface of composite containing 9.1 wt% MWCNT and (d) bottom surface of composite containing 9.1 wt% MWCNT.

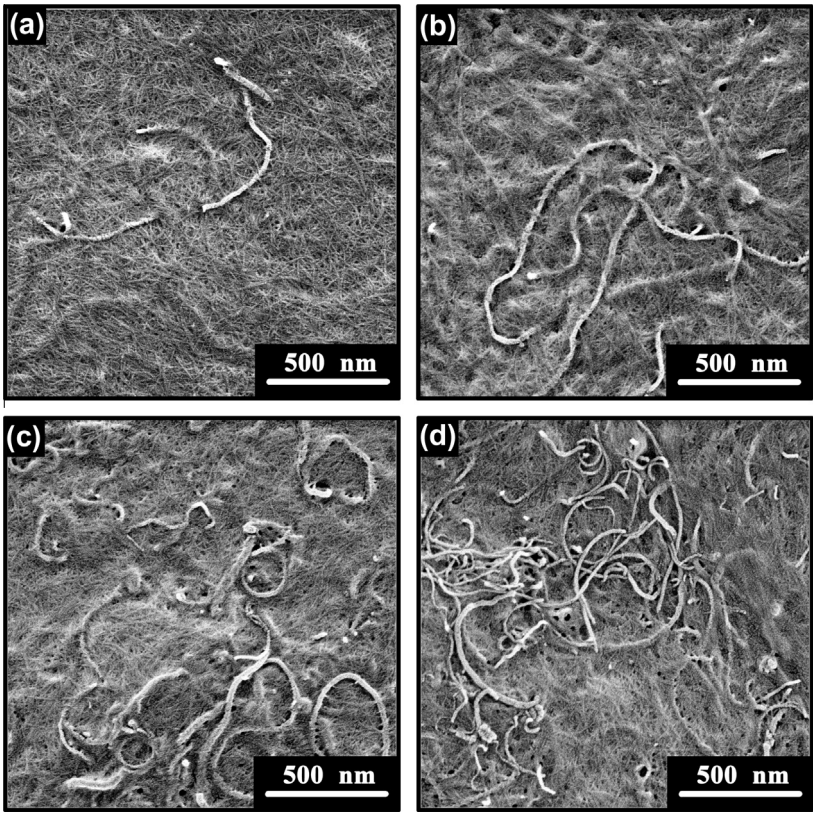

Fig. 4. Morphology of nanopaper at different concentrations of MWCNT in NFC by weight: (a) 2.0 wt%, (b) 5.7 wt%, (c) 9.1 wt% and (d) 16.7 wt%.

Fig. 2 (FE-SEM) and Fig. 3 (AFM). Pure NFC nanopaper showed a random-in-plane weblike network structure of cellulose nanofibrils of uniform width (Figs. 2a and 3a). The NPPE modified MWCNT were well individualized in water and a fibrous network was obtained after drying (Figs. 2b and 3b). The width of MWCNT was estimated to be 3–4 times higher than the NFC nanofibrils (Fig. 2a and b). The lengths of both NFC and MWCNT are possibly several micrometers and nanofibril ends are not apparent. The typical top (Figs. 2c and 3c) and bottom surfaces (Figs. 2d and 3d) of the NFC/CNT nanopaper with 9.1 wt% MWCNT indicated homogenous incorporation of MWCNT in the cellulose nanofibril network. The organization of both cellulose nanofibrils and MWCNT is random-in-the-plane of swirled fibrils.

The FE-SEM images of the NFC/CNT nanopaper samples containing different amounts of MWCNT are compared in Fig. 4. MWCNT are individually dispersed in the NFC network with or without very few contacts between each other in the sample with 2.0 wt% MWCNT (Fig. 4a). The number of contacts between the MWNCTs increased at 5.7 wt% MWCNT loading (Fig. 4b), while a continuous MWCNT network is formed at 9.1 wt% MWCNT (Fig. 4c). However, at 16.7 wt% MWCNT loading, agglomerates of MWCNT are observed (Fig. 4d).

These structural observations show homogeneous nanopaper structures based on NFC and CNT prepared from mixed water suspensions using NPPE surfactant. We are aware of the need to reduce the use of NPPE surfactant due to its possible negative effect on living organisms [40,41]. Testing of other surfactants with similar hydrophilic–lipophilic balance as NPPE is in progress.

3.2. Mechanical properties

The stress–strain behaviour in uniaxial tension of the NFC/CNT samples is presented in Fig. 5. Associated property data and the standard deviations are in Table 1. At low strains (<1%) the stress–strain behaviour is linear elastic. At a stress in the region of 90–120 MPa, there is a knee in the curve (apparent yield stress $\sigma_{0.2}$) followed by a linear and fairly strongly strain-hardening plastic region [42]. The slope of the linear elastic region of the curves corresponds to the Young's modulus, which is 9.26 GPa despite an estimated porosity of 40%. It is well known that the porosity has significant effect on the mechanical properties of cellulose nanopaper. It was suggested that the porosity of the nanopaper increases with introduction of surface charge on the cellulose nanofibrils [43]. Nanopaper prepared from nanofribrils isolated using mild enzymatic treatment having almost no surface charge exhibit porosity in the range of 20–28% [42], whereas nanopapers prepared from surface quaternized nanofibrils show increased porosities (37–48%) dependent on the surface charge (0.59–2.31 mmol/g) respectively [43].

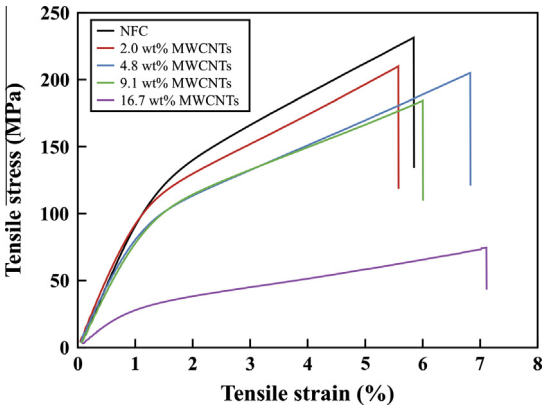

Fig. 5. Typical stress–strain curves of NFC/MWCNT nanopaper at different MWCNT content.

There is slight decrease in the Young's modulus with increasing concentration of MWCNT. The same behaviour is observed for the tensile strength of the material. There was a significant decrease in the strain to failure at very low MWCNT loading (0.5–1 wt%). However, at MWCNT loading higher than 2 wt%, the strain to failure increases back to its original value and does not change significantly. At 7.4 wt% CNT, the strength is 210 MPa and strain to failure 7.2%. These high values are due to the strength of the NFC network itself but are still remarkably high considering the high porosity. No positive contribution from the CNT is observed in Table 1, since the interaction with NFC is weak or non-existing.

The strain at which the yield phenomenon occurs decreases with increasing MWCNT content. It was suggested [42] that yielding is associated with onset of irreversible interfibril debonding and NFC slippage facilitated by voids. Pores could also explain the slight decrease in strength of the composites with increasing MWCNT content, since the porosity of the nanopaper increases with increasing MWCNT concentration (Table 1) as well. Increased porosity with increased MWCNT content must be related to reduced capillary effects between NFC fibrils during drying. NFC fibrils interact less during drying due to the presence of MWCNT, and the porosity becomes higher. However, it should be emphasized that nanopaper maintains mechanical properties fairly well up to 9.1 wt% of MWCNT. The material keeps its flexibility and toughness and in comparison withplastics, glass, ceramics and metals it is lightweight and can be easily folded. The lack of positive contribution of MWCNT to NFC properties must be related to poor stress-transfer due to weak molecular interactions between the two constituents. In the study by Koga et al. [32], the strength values are higher than in the present study. It is not straightforward to compare those with the present data since Koga et al. tested very thin films of materials likely to show thickness-dependent strength. Most likely, the porosity of the present materials promotes the favorable performance observed in terms of yielding, ductility and toughness (work to fracture).

3.3. Electrical conductivity

The electrical conductivity (resistivity) of a composite is strongly dependent on the volume fraction of the conductive phase.

Fig. 6a shows the static values of the DC conductivity of NFC/CNT nanopapers with different amounts of MWCNT at two different sample thicknesses (25 and 50 μm). At low volume fractions and low connectivity, the conductivity remains very close to the conductivity of the matrix, in this case neat NFC nanopaper. The percolation composition (p_c) clearly occurs between 6 and 9 wt%. At this composition, the conductivity changes significantly (over more than 4 decades). In other words, below this concentration the composites are very resistant to electrical flow, whereas above this value the composites are conductive. Depending on the matrix, the processing technique and the CNT type used, percolation thresholds ranging from 0.001 wt% to more than 10 wt% have been reported [44]. Similar percolation thresholds were observed previously for the conductive paper prepared from SWCNT and bleached hardwood kraft pulp fiber [20].

Dependence of DC conductivity (σ_{DC}) on filler content (p) near the percolation threshold p_c can be described by power law $\sigma_{DC}(p) \approx (p - p_c)^t$ above the percolation threshold ($p > p_c$). In order to get an estimate for p_c and the critical exponent t; we fitted the σ_{DC} data for $p > p_c$. This was done by variation of p_c in the interval from 6 to 8 in steps of 0.5. For each value of p_c the value of t has been determined from the slope of the linear relation of σ_{DC} and

Table 1
Average physical and mechanical properties of conductive nanopaper (the standard deviations are in parentheses).

MWCNT content (wt%)	Density (kg/m^3)	Porosity (%)	MWCNT content (vol%)	Young's modulus E (GPa)	Tensile strength σ (MPa)	Strain to failure ε (%)
0	0.889	40.7	0.0	9.26 (0.43)	239 (23.0)	6.2 (0.9)
0.5	0.850	43.4	0.2	9.34 (0.57)	177 (21.0)	3.6 (0.7)
1.0	0.906	39.8	0.4	9.15 (0.65)	199 (35.0)	4.8 (1.2)
2.0	0.960	36.5	0.9	8.78 (0.33)	212 (8.6)	6.1 (0.4)
4.8	0.848	44.5	1.9	8.54 (0.43)	208 (13.0)	6.5 (1.0)
5.7	0.859	44.0	2.3	8.25 (0.27)	205 (13.0)	6.6 (0.8)
7.4	0.823	46.7	2.9	7.54 (0.22)	210 (15.0)	7.2 (0.6)
9.1	0.820	47.3	3.5	7.72 (0.24)	183 (8.7)	6.0 (0.4)
16.7	0.731	54.3	5.8	2.60 (0.16)	66.2 (8.3)	6.9 (1.1)

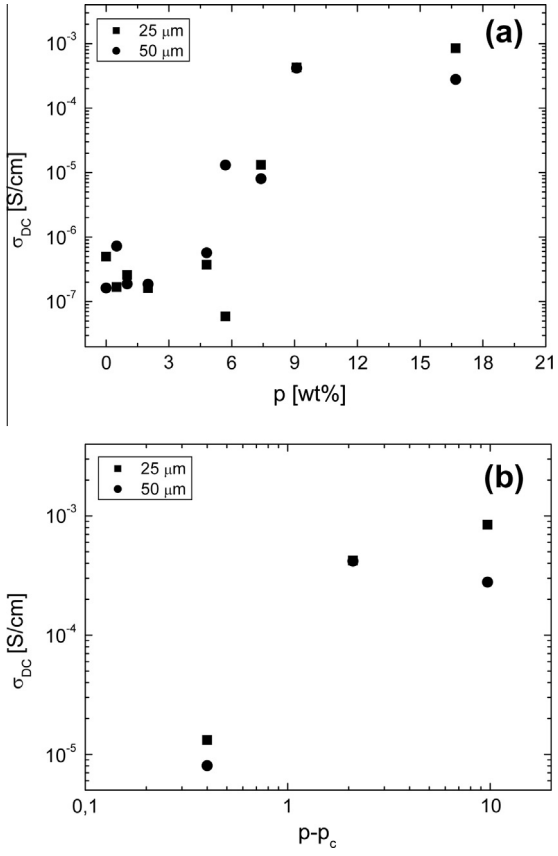

Fig. 6. (a) DC conductivity σ_{DC} versus MWCNT concentration p (wt%) for the prepared samples. (b) Values of σ_{DC} above the percolation concentration p_c versus $(p–p_c)$.

$p–p_c$ on a log–log scale. The lowest value of the root mean square error was found for $p_c = 7$ with the exponent $t = 1.5$ (Fig. 6b).

The value $t = 1.5$ calculated here for the MWCNT composites is in good agreement with the theoretical value of $t \approx 2$ for a percolation network in three dimensions [45–49]. This, however, does not exclude the existence of aggregates or bundles of CNT.

4. Conclusions

A simple and environmentally friendly method has been developed for preparation of lightweight and electrically conductive nanopaper structures. The strength and toughness of cellulose nanofibril networks is combined with the electrical conductivity of carbon nanotube networks in commingled nanopaper structures. NFC cellulose nanofibrils were mixed with NPPE surfactant modified MWCNT to form a stable aqueous suspension. A paper-making approach was used to form the commingled nanopaper structures without the use of organic solvents or other chemical modification. For the present hydrocolloidal mixtures, the purpose of CNT surface treatment is not only to provide CNT dispersion in water. The purpose is also to ensure a homogeneous NFC/CNT suspension mixture. The surfactant thus also acts as a compatibilizer in the colloidal state.

Most existing preparation methods for CNT nanocomposites allow only low volume fractions of CNT. The present approach resulted in a nonwoven nanopaper structure with 9.1 wt% of CNT. The tensile strength for this composition was 183 MPa and the strain to failure 6%, due to the load-bearing function of the NFC network. The electrical conductivity of this NFC/CNT nanopaper composition increased 4 orders of magnitude compared with neat NFC nanopaper, since a continuous percolated MWCNT phase was formed. Most likely, the surfactant had a negative effect on the percolation threshold concentration of CNT by possible formation of insulating layer around the CNT [50]. The porous NFC/CNT nanopaper structure is mechanically favorable in that it allows a combination of high strength and toughness in tension, combined with high flexibility in bending. The flexibility is a consequence of nanopaper porosity (40–55%) combined with the fine dimensions and high strengths of NFC and CNT (can be bent to small radius of curvature without fracture). The present papermaking concept for CNT materials provides green water-based processing, and potential upscaling to industrial processing of large material volumes with high CNT content. This provides potential for high electrical conductivity at preserved mechanical performance. The material can be cast as thin coatings, as thicker free-standing films or as moulded structures of complex geometrical shape.

Acknowledgment

Wallenberg Wood Science Center is gratefully acknowledged for financial support.

References

[1] Berglund LA, Peijs T. Cellulose biocomposites-from bulk moldings to nanostructured systems. MRS Bull 2010;35(3):201–7.
[2] Eichhorn SJ et al. Review: current international research into cellulose nanofibres and nanocomposites. J Mater Sci 2010;45(1):1–33.
[3] Klemm D et al. Nanocelluloses: a new family of nature-based materials. Angew Chem-Int Ed 2011;50(24):5438–66.
[4] Wagberg L et al. The build-up of polyelectrolyte multilayers of microfibrillated cellulose and cationic polyelectrolytes. Langmuir 2008;24(3):784–95.
[5] Saito T et al. Homogeneous suspensions of individualized microfibrils from TEMPO-catalyzed oxidation of native cellulose. Biomacromolecules 2006;7(6):1687–91.
[6] Saito T et al. Cellulose nanofibers prepared by TEMPO-mediated oxidation of native cellulose. Biomacromolecules 2007;8(8):2485–91.
[7] Saito T et al. Individualization of nano-sized plant cellulose fibrils by direct surface carboxylation using TEMPO catalyst under neutral conditions. Biomacromolecules 2009;10(7):1992–6.
[8] Pei AH et al. Surface quaternized cellulose nanofibrils with high water absorbency and adsorption capacity for anionic dyes. Soft Matter 2013;9(6):2047–55.

[9] Zhou Q et al. Nanostructured biocomposites based on bacterial cellulosic nanofibers compartmentalized by a soft hydroxyethylcellulose matrix coating. Soft Matter 2009;5(21):4124–30.
[10] Sehaqui H, Zhou Q, Berglund LA. Nanostructured biocomposites of high toughness-a wood cellulose nanofiber network in ductile hydroxyethylcellulose matrix. Soft Matter 2011;7(16):7342–50.
[11] Henriksson M et al. An environmentally friendly method for enzyme-assisted preparation of microfibrillated cellulose (MFC) nanofibers. Eur Polymer J 2007;43(8):3434–41.
[12] Paakko M et al. Enzymatic hydrolysis combined with mechanical shearing and high-pressure homogenization for nanoscale cellulose fibrils and strong gels. Biomacromolecules 2007;8(6):1934–41.
[13] Sehaqui H et al. Wood cellulose biocomposites with fibrous structures at micro- and nanoscale. Compos Sci Technol 2011;71(3):382–7.
[14] Sehaqui H et al. Fast preparation procedure for large, flat cellulose and cellulose/inorganic nanopaper structures. Biomacromolecules 2010;11(9):2195–8.
[15] Liu AD et al. Clay nanopaper with tough cellulose nanofiber matrix for fire retardancy and gas barrier functions. Biomacromolecules 2011;12(3):633–41.
[16] Liu A, Berglund LA. Clay nanopaper composites of nacre-like structure based on montmorrilonite and cellulose nanofibers-improvements due to chitosan addition. Carbohydr Polym 2012;87(1):53–60.
[17] Li D et al. Processable aqueous dispersions of graphene nanosheets. Nat Nanotechnol 2008;3(2):101–5.
[18] Zhang M et al. Strong, transparent, multifunctional, carbon nanotube sheets. Science 2005;309(5738):1215–9.
[19] Toomadj F, Farjana S, Sanz-Valesco A, Naboka O, Lundgren P, Rodriguez K, et al. Strain sensitivity of carbon nanotubes modified cellulose. Proc Eng 2011;25:1353–6.
[20] Anderson RE et al. Multifunctional single-walled carbon nanotube-cellulose composite paper. J Mater Chem 2010;20(12):2400–7.
[21] Xiao L et al. Flexible, stretchable, transparent carbon nanotube thin film loudspeakers. Nano Lett 2008;8(12):4539–45.
[22] Fugetsu B et al. Electrical conductivity and electromagnetic interference shielding efficiency of carbon nanotube/cellulose composite paper. Carbon 2008;46(9):1256–8.
[23] Oya T, Ogino T. Production of electrically conductive paper by adding carbon nanotubes. Carbon 2008;46(1):169–71.
[24] Jung R et al. Electrically conductive transparent papers using multiwalled carbon nanotubes. J Polymer Sci Part B – Polymer Phys 2008;46(12):1235–42.
[25] Kim Y et al. Transparent conducting films based on nanofibrous polymeric membranes and single-walled carbon nanotubes. J Appl Polym Sci 2009;114(5):2864–72.
[26] Farjana S, Toomadj F, Lundgren P, Sanz-Velasco A, Naboka O, Enoksson P. Conductivity-dependent strain response of carbon nanotube treated bacterial nanocellulose. J Sensors 2013.
[27] Yan ZY et al. Cellulose synthesized by acetobacter xylinum in the presence of multi-walled carbon nanotubes. Carbohydr Res 2008;343(1):73–80.
[28] Park WI et al. Synthesis of bacterial celluloses in multiwalled carbon nanotube-dispersed medium. Carbohydr Polym 2009;77(3):457–63.
[29] Zhang H et al. Regenerated-cellulose/multiwalled-carbon-nanotube composite fibers with enhanced mechanical properties prepared with the ionic liquid 1-allyl-3-methylimidazolium chloride. Adv Mater 2007;19(5):698.
[30] Yun S, Kim J. Characteristics and performance of functionalized MWNT blended cellulose electro-active paper actuator. Synth Met 2008;158(13):521–6.
[31] Salajková M. Nanocelluloses – surface modification and use in functional materials. Licentiate Thesis 2012.
[32] Koga H et al. Transparent, conductive, and printable composites consisting of TEMPO-oxidized nanocellulose and carbon nanotube. Biomacromolecules 2013.
[33] Chen XH et al. Non-destructive purification of multi-walled carbon nanotubes produced by catalyzed CVD. Mater Lett 2002;57(3):734–8.
[34] Baggerund E, Lindström T. Measurement of volume fractions of solid, liquid and gas in kraft and CTMP paper at varying moisture content. In: Proceedings of the international paper, physics conference; 2003. p. 157–63.
[35] Hussein L, Krüger M. Fabrication and characterization of buckypaper-based nanostructured electrodes as a novel material for biofuel cell applications. Phys Chem Chem Phys 2011;13:5831–9.
[36] Heux L, Chauve G, Bonini C. Nonflocculating and chiral-nematic self-ordering of cellulose microcrystals suspensions in nonpolar solvents. Langmuir 2000;16(21):8210–2.
[37] Bonini C et al. Rodlike cellulose whiskers coated with surfactant: a small-angle neutron scattering characterization. Langmuir 2002;18(8):3311–4.
[38] Ljungberg N et al. New nanocomposite materials reinforced with cellulose whiskers in atactic polypropylene: effect of surface and dispersion characteristics. Biomacromolecules 2005;6(5):2732–9.
[39] Bondeson D, Oksman K. Dispersion and characteristics of surfactant modified cellulose whiskers nanocomposites. Compos Interfaces 2007;14(7–9):617–30.
[40] Shang DY, Macdonald RW, Ikonomou MG. Persistence of nonylphenol ethoxylate surfactants and their primary degradation products in sediments from near a municipal outfall in the strait of Georgia, British Columbia, Canada. Environ Sci Technol 1999;33(9):1366–72.
[41] Ying GG, Williams B, Kookana R. Environmental fate of alkylphenols and alkylphenol ethoxylates – a review. Environ Int 2002;28(3):215–26.
[42] Henriksson M et al. Cellulose nanopaper structures of high toughness. Biomacromolecules 2008;9(6):1579–85.
[43] Pei AB, Nuria, Berglund Lars, Zhou Qi. Surface quaternized cellulose nanofibrils with high water absorbency and adsorption capacity for anionic dyes. Soft Matter 2012.
[44] Li C, Thostenson ET, Chou TW. Sensors and actuators based on carbon nanotubes and their composites: a review. Compos Sci Technol 2008;68(6):1227–49.
[45] Fisch R, Harris AB. Critical behavior of random resistor networks near percolation threshold. Phys Rev B 1978;18(1):416–20.
[46] Adler J et al. Low-concentration series in general dimension. J Stat Phys 1990;58(3–4):511–38.
[47] Adler J. Conductivity exponents from the analysis of series expansions for random resistor networks. J Phys a-Math General 1985;18(2):307–14.
[48] Alexander S, Orbach R. Density of states on fractals – fractons. J De Phys Lett 1982;43(17):L625–31.
[49] Gingold DB, Lobb CJ. Percolative conduction in 3 dimensions. Phys Rev B 1990;42(13):8220–4.
[50] Hermant MC et al. Lowering the percolation threshold of single-walled carbon nanotubes using polystyrene/poly(3,4-ethylenedioxythiophene): poly(styrene sulfonate) blends. Soft Matter 2009;5(4):878–85.